

Orbital Magnetic Moment Instability at the Spin Reorientation Transition of $\text{Nd}_2\text{Fe}_{14}\text{B}$

L. M. García, J. Chaboy, and F. Bartolomé

Instituto de Ciencia de Materiales de Aragón and Departamento de Física de la Materia Condensada, CSIC-Universidad de Zaragoza, Facultad de Ciencias, E. 50009, Zaragoza, Spain

J. B. Goedkoop

Faculty of Mathematics, Computer Science, Physics and Astronomy, University of Amsterdam, Valckenierstraat 65, NL-1018 XE Amsterdam, The Netherlands

(Received 4 February 2000)

Highly accurate soft-XMCD data recorded on a $\text{Nd}_2\text{Fe}_{14}\text{B}$ single crystal, through the spin reorientation transition show that the average Fe orbital moment (a) is proportional to the macroscopic Fe anisotropy constant, and (b) diverges 15 K below the reorientation transition temperature. This divergence is indicative of a critical behavior and it is related to a tetragonal distortion. These results give experimental evidence of the mutual dependence between orbital moment, macroscopic magnetic anisotropy, and tetragonal distortion. Furthermore, it is argued that the critical behavior of the orbital moment is at the origin of similar divergences previously observed in Mössbauer and Hall-effect data.

PACS numbers: 78.70.Dm, 75.25.+z, 75.40.-s

Strong x-ray magneto-optical effects at atomic absorption resonances have opened new pathways for the study of magnetism. In particular, x-ray absorption spectroscopy (XAS) with circularly polarized x-ray beams has yielded a simple tool for the study of elemental sublattice magnetizations in the form of x-ray magnetic circular dichroism (XMCD) [1,2]. The sum rules [3,4] for XMCD offer the possibility to separately determine spin- and orbital magnetic moments. Exceptionally interesting results have been reported on the change of the orbital magnetic moment of transition metals observed in low-dimensional structures like surfaces [5], multilayers [6], and nanoscale clusters [7] with respect to the bulk values. These results reveal that the orbital magnetic moment of transition metals is very sensitive to the symmetry of the local environment. Furthermore, XMCD studies have highlighted the close relationship between the orbital moment and the macroscopic magnetocrystalline anisotropy (MCA) [8–10]. These findings are in agreement with the simple Bruno's model [11], which shows that if the majority spin band is completely filled (i.e., a hard ferromagnet) the MCA is proportional to the orbital magnetization. Band-structure calculations for face-centered-tetragonal (fct) Ni confirm this picture, showing also a near proportionality between the orbital magnetization and the tetragonal distortion of this system [12]. Therefore it can be said that the orbital moment links the lattice structure and the macroscopic magnetic anisotropy.

At many magnetic phase transitions, magnetic and structural parameters change in a correlated way. A model for such transitions is the spin reorientation transition (SRT) in $\text{Nd}_2\text{Fe}_{14}\text{B}$. This material has been studied extensively because of its technological importance as the best performing permanent magnet [13], and as a result this compound has become one of the prototypes of rare-earth-transition metal intermetallic compounds. In these systems, itinerant

$3d$ electrons of the transition metal with orbital moments that are almost totally quenched by the crystal electric field coexist with localized $4f$ electrons of the rare earth with orbital moments that retain their atomic values.

At high temperatures, both the iron and neodymium magnetocrystalline anisotropies are uniaxial and the magnetization in $\text{Nd}_2\text{Fe}_{14}\text{B}$ points at the [001] direction (c axis). In fact, the MCA of the Fe moments is uniaxial in the whole temperature range, and its corresponding energy may be expressed appropriately as $E_a^{\text{Fe}} = K_1^{\text{Fe}} \sin^2 \theta$, where θ is the angle between the magnetization and the c axis and K_1^{Fe} is positive and temperature dependent [13]. However, the MCA of the Nd moments is more complex. Indeed, the higher order terms of the crystal electric field of the Nd sites force the rotation ($T_{\text{SRT}} = 135$ K) of the total magnetization from the [001] direction towards the [110] axis, reaching a tilting angle of 30.6° at 4.2 K [14]. This spin reorientation transition is accompanied by strong magnetoelastic effects [15,16].

This situation renders this magnetic phase transition particularly interesting for the study of the quenching of orbital moments. With this aim, we have performed XMCD measurements on a $\text{Nd}_2\text{Fe}_{14}\text{B}$ single crystal as a function of temperature through the SRT [14]. We find the existence of a direct correlation between the iron magnetocrystalline anisotropy constant K_1^{Fe} , the orbital moment of the Fe sublattice, and the tetragonal distortion of $\text{Nd}_2\text{Fe}_{14}\text{B}$ over the whole temperature range studied (4–290 K), in agreement with the theoretical predictions [11,12]. The existence of a strong instability in the iron orbital magnetic moment occurring ~ 15 K below T_{SRT} is demonstrated, while no such anomalous behavior is observed in the spin moment. We interpret this instability as critical behavior of the orbital moment.

X-ray absorption measurements at the Fe $L_{2,3}$ ($2p \rightarrow 3d$ transitions) and at the Nd $M_{4,5}$ ($3d \rightarrow 4f$ transitions)

edges were carried out at fixed temperatures between 4.2 and 290 K on the Dragon beam line (ID12B) at the European Synchrotron Radiation Facility [17]. The measured rate of circular polarization is $P_c = (84 \pm 5)\%$ at the Fe edges and $P_c = (90 \pm 5)\%$ at the Nd edges [18]. The crystal was mounted with the c axis parallel to the light propagation direction and the magnetic field. To prepare a clean surface, the crystal was cleaved *in situ* at a pressure of 1×10^{-9} mbar. The spectra were acquired by measuring the drain current as a function of photon energy, which is a surface sensitive method. The pressure in the cryomagnet chamber during the 36 hours of measurement was kept at 1×10^{-10} mbar and no signs of surface degradation were observed over this period. XAS spectra $I^{+(-)}$ were recorded by applying a magnetic field of 1 T, enough to saturate the magnetization, (anti-)parallel to the light propagation direction. In this geometry, $L_{2,3}$ and $M_{4,5}$ XMCD probes the average Fe-3d and Nd-4f magnetic moments projected along the c axis. The XMCD spectra presented here are the averages of differences $I^+ - I^-$ between two consecutive spectra recorded at opposite field directions. In this experimental setup angular saturation effects [19,20] intrinsic to the TEY detection are negligible.

Figure 1 shows a typical example of the normalized Fe $L_{2,3}$ -edge XAS and XMCD spectra, taken at 290 K. In the case of the $L_{2,3}$ edges of Fe the orbital and the spin magnetic moments can be determined from the XMCD spectrum according to [3,4,21]:

$$m_L = -\frac{4}{3P_c} \frac{\int_{L_2+L_3} (I^+ - I^-) d\omega}{\int_{L_2+L_3} (I^+ + I^-) d\omega} (10 - n_{3d})$$

$$= -\frac{2q}{3P_c r} (10 - n_{3d}), \quad (1)$$

$$m_S = -\frac{1}{P_c} \frac{6 \int_{L_3} (I^+ - I^-) d\omega - 4 \int_{L_2+L_3} (I^+ - I^-) d\omega}{\int_{L_2+L_3} (I^+ + I^-) d\omega} \times (10 - n_{3d})$$

$$= -\frac{3p - 2q}{P_c r} (10 - n_{3d}), \quad (2)$$

where m_L and m_S are in units of μ_B/atom , n_{3d} is the 3d electron occupation number of Fe. As usual, the unpolarized 3d spectral weight in the denominator is approximated by $[I^+(\omega) + I^-(\omega)]/2$. To evaluate its integral r , the non-3d contributions to the spectra have to be removed. We approximated these contributions by two Heaviside step functions centered at the L_3 and L_2 absorption maxima with an intensity ratio of 2:1 according to the degeneracy of the $2p$ core hole, $2j + 1$, and normalized to the average intensity of the last 20 eV of the spectra. The XMCD integral for the whole energy range q can be precisely determined. The p value is the integrated XMCD value at the onset of the L_2 white line. Because of the overlap of the L_3 and L_2 multiplets this procedure tends to systematically underestimate p by $\sim 10\%$. For n_{3d} , we used the value of 6.45 ± 0.05 determined from band structure calculations [22,23].

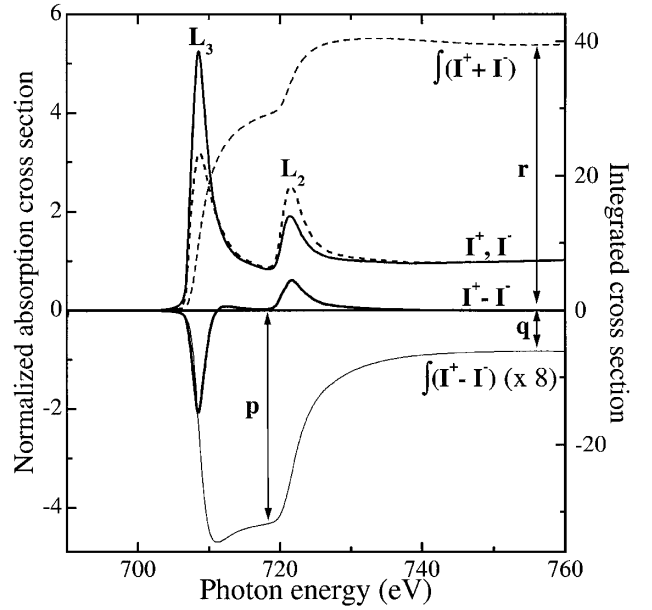


FIG. 1. XAS spectra of $\text{Nd}_2\text{Fe}_{14}\text{B}$ at 290 K. I^+ (I^-) are the normalized XAS spectra for (anti)parallel magnetic field and light helicity. $I^+ - I^-$ indicates the XMCD spectrum. Its integral is plotted versus the right-hand scale, as is the integral of the background-subtracted average of the I^+ and I^- spectra. The values p , q , and r are the parameters needed in the sum-rule analysis.

Applying Eqs. (1) and (2) to the $T = 290$ K spectra of Fig. 1, we obtain $m_L = 0.107 \pm 0.005 \mu_B$ and $m_S = 2.16 \pm 0.10 \mu_B$, giving a total magnetic moment $m_{\text{XMCD}}^{\text{Fe}} = 2.27 \pm 0.11 \mu_B$. The systematic error in the absolute values is estimated at about 10%, but the relative error between temperatures is not larger than 3%–4%. The XMCD-derived total moment agrees satisfactorily with the values determined by other techniques: polarized neutron diffraction: $2.20 \mu_B$ [24], Mössbauer spectroscopy: $2.00 \mu_B$ [25], band structure calculations: $2.35 \mu_B$ [22,23]. There are no previous experimental determinations for the orbital magnetic moment, but our value is in agreement with the $\leq 0.1 \mu_B$ suggested by Fruchart [26] from Mössbauer measurements. It is somewhat larger than the $0.06 \mu_B$ computed by band structure calculations for this compound [23], and 20% higher than has been measured in bcc-Fe ($0.08 \mu_B$) [21].

Figure 2 shows the temperature dependence of the XMCD-derived moments m_L , m_S , and $m_{\text{XMCD}} = m_L + m_S$ which reflects the projection of the Fe moment along the c axis. Also shown is the modulus of the Fe moment, determined from ^{57}Fe Mössbauer spectroscopy [25]. At $T > T_{\text{SRT}}$ the two datasets agree quantitatively to within the experimental uncertainty. Below the reorientation transition the averaged angular distribution of the Fe moments with respect to the c axis, $\theta_{\text{Fe}}(T)$ can be obtained from the simple formula [27] $\cos \theta_{\text{Fe}} = m_{\text{XMCD}}/m_{\text{Möss}}$. The $\theta_{\text{Fe}}(T)$ curve obtained with this method, shown in Fig. 3(a), is in excellent agreement with that determined from Mössbauer measurements [25].

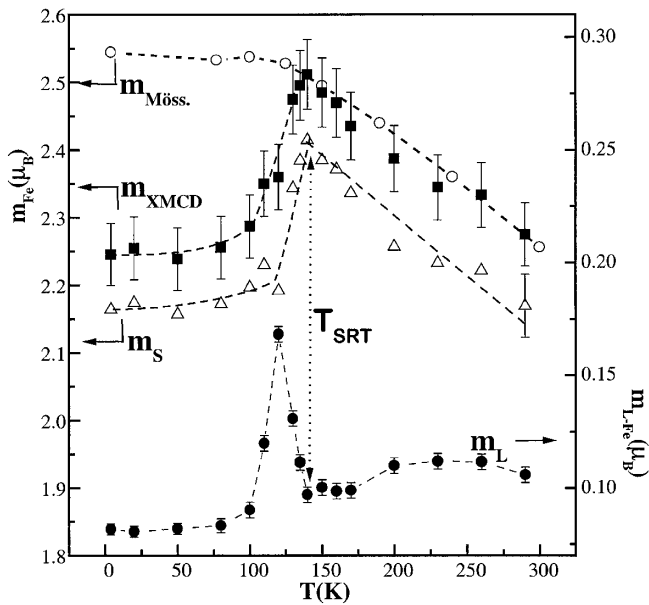


FIG. 2. Temperature dependence of c -axis projected orbital, spin, and total Fe magnetic moment derived from sum-rules analysis. Data for the Fe magnetic moment modulus obtained from ^{57}Fe Mössbauer spectroscopy from Ref. [25] are also shown.

Beyond the quantitative determination of the orbital and spin moments and tilting angles of iron moments, the most striking aspect of the data in Fig. 2 is the behavior of the orbital moment. It can be described as a slow increase with temperature to a broad maximum at 230 K, on which is superimposed a sharp peak centered around 120 K (15 K below T_{SRT}), where the orbital moment reaches twice the low temperature value. This behavior is in sharp contrast to that of the spin moment which does not show any anomaly at 120 K, but only a reduction in the projection of the iron spin along the c axis, associated with the rotation of the Fe moments [25]. This peculiar behavior of iron orbital moment is in contrast to that observed for Nd. Indeed, at all temperatures we also measured the Nd $M_{4,5}$ XMCD spectra. Since in these spectra the overlap between the spin-orbit split M_5 and M_4 edges is much stronger than in Fe, the spin sum rule [4] cannot be used quantitatively. However, using the sum rules *qualitatively* we determined [28] that m_L/m_S of the Nd $4f$ shell remains constant over the whole temperature range to within the experimental error of 5%, in clear contrast with the large orbital instability observed in the Fe $3d$ shell.

The question is how the orbital moment relates to the anisotropy constant of the Fe sublattice K_1^{Fe} . K_1^{Fe} in $\text{Nd}_2\text{Fe}_{14}\text{B}$ cannot be measured directly since the total anisotropy constant is dominated by the Nd contribution [13]. However, it has been estimated from magnetization measurements of the sister compound $\text{Y}_2\text{Fe}_{14}\text{B}$ [29], reproduced in Fig. 3(b) versus reduced temperature T/T_c . Measurement of K_1^{Fe} of $\text{R}_2\text{Fe}_{14}\text{B}$ compounds with R atoms with zero orbital moment ($R = \text{Y, La, Gd, Lu}$) has revealed a universal anomalous behavior in all compounds,

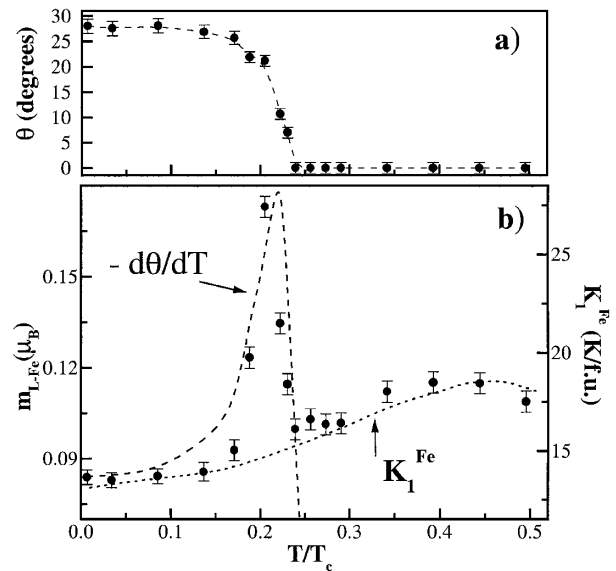


FIG. 3. (a) Temperature dependence of the order parameter (canting angle of the magnetization away from the c axis). (b) orbital moments from Fig. 2 compared with the scaled derivative of the order parameter (dash) and the macroscopic anisotropy of $\text{Y}_2\text{Fe}_{14}\text{B}$ (dot) (Ref. [29]), all plotted versus reduced temperature T/T_c , T_c ($\text{Y}_2\text{Fe}_{14}\text{B}$) = 565 K, T_c ($\text{Nd}_2\text{Fe}_{14}\text{B}$) = 585 K.

with a broad maximum at $T/T_c = 0.45$ [29]. From the comparison with the orbital moment in Fig. 3(b), we show here experimentally that the Fe orbital moment is *exactly proportional* to K_1^{Fe} over the whole temperature range, except for the peak below T_{SRT} . Bolzoni *et al.* [29] already correlated the temperature dependence of K_1^{Fe} with the tetragonal (c/a) distortion that $\text{Nd}_2\text{Fe}_{14}\text{B}$ exhibits ($K_1 = M^3[1-0.52(c/a)^2]$). We conclude that the relationship between K_1^{Fe} , m_L and the tetragonal lattice distortion, as was predicted by theory [12], is experimentally confirmed to be a good first order approximation.

Turning to the interpretation of the peak in m_L at SRT, if the anomalous behavior of m_L were due to the change in the magnetic symmetry at the SRT (from uniaxial at high temperature to canted at low temperature), one would expect a step rather than a peak as has indeed been observed in the Nd moment [25] and in the unit cell volume [15]. One notices from comparison with Fig. 3(a) that the peak corresponds with the temperature range in which the order parameter $\theta(T)$ is turning. To make the relationship more precise, we fitted a spline curve to the order parameter and plot the derivative of this fit in Fig. 3(b) (with reversed sign). Obviously the peak in the orbital moment is nearly proportional to the rate of change of the order parameter $d\theta(T)/dT$. Hence, the orbital instability is intrinsically associated to the critical dynamics of the phase transition.

The question is whether the peak in the orbital moment can be related with similar behavior of K_1^{Fe} and/or a tetragonal distortion even at the anomalous peak. For the former there are no data for the reasons explained above. For the latter, high field magnetostriction data exist [16]

that show a clear divergence in the tetragonal distortion, just below the SRT and centered at 110 ± 10 K. Its origin remained unclear in the original work but with the proportionality of m_L and the tetragonal distortion in mind, now also it can be interpreted as critical behavior.

Similar anomalies in the critical temperature region have been reported in the literature. ^{57}Fe Mössbauer data [25] show a pronounced anomaly in the isomer shifts of all six Fe sites, superimposed on a step between the high and low temperature phases. Such shifts reflect changes in the electronic density at the nucleus but are difficult to interpret [30]. However, the hyperfine field likewise shows a 1% anomaly at the same temperatures. It has an orbital contribution from the $3d$ electrons that is proportional to the orbital moment, which for bcc Fe is about 1% [31]. A doubling of the orbital moment as observed here explains the anomaly in H_{hyp} . Second, Hall resistivity data have been published very recently [32] that likewise show a peak similar to that observed here. It has been interpreted as a critical behavior of the skew scattering mechanism, that is a result of the spin-orbit interaction $\mathbf{l} \cdot \mathbf{s}$ [33]. In this picture, a doubling of the orbital moment naturally explains the Hall effect behavior.

In conclusion, we have experimentally demonstrated the existence of a mutual dependence between the iron-sublattice anisotropy constant, the iron orbital magnetic moment, and the tetragonal lattice distortion as a function of temperature in the whole temperature range. This relationship is fulfilled even at the spin reorientation phase transition, where we have observed a large and sharp instability in the iron orbital moment, intrinsically associated with the dynamics of the order parameter. To our knowledge, this is the first evidence for an orbital instability at a magnetic phase transition. The critical behavior in the orbital moment can be considered as the missing link between the Nd-spin reorientation that drives the transition and the resulting magnetostriction anomaly on the one hand and the critical behavior of the Mössbauer hyperfine data and Hall effect data on the other.

This work was partially supported by the Spanish DGICYT Projects No. MAT99-0667-C04-04 and No. MAT97-0987. We thank H. Maruyama for useful discussions and M. Sagawa for providing the single crystal. We gratefully acknowledge the help of N. B. Brookes, M. Finazzi, and K. Larsson during the experimental work at the European Synchrotron Radiation Facility (Proposal No. HE-143).

[1] G. Schütz *et al.*, Phys. Rev. Lett. **58**, 737 (1987); C. T. Chen *et al.*, Phys. Rev. B **42**, 7262 (1990); T. Koide *et al.*, *ibid.* **44**, 4697 (1991).

[2] J. Stöhr and H. Köning, Phys. Rev. Lett. **75**, 3748 (1995); L. M. García *et al.*, J. Appl. Phys. **79**, 6497 (1996); W. Grange *et al.*, J. Appl. Phys. **83**, 6617 (1998); J. Chaboy *et al.*, Phys. Rev. B **57**, 8424 (1998).

[3] B. T. Thole *et al.*, Phys. Rev. Lett. **68**, 1943 (1992).

[4] P. Carra *et al.*, Phys. Rev. Lett. **70**, 694 (1993).

[5] R. Wu *et al.*, J. Magn. Magn. Mater. **132**, 103 (1994).

[6] J. Vogel *et al.*, Phys. Rev. B **55**, 3663 (1997).

[7] K. W. Edmonds *et al.*, Phys. Rev. B **60**, 472 (1999); H. A. Dürr *et al.*, Phys. Rev. B **59**, R701 (1999).

[8] J. Stöhr and H. Köning, Phys. Rev. Lett. **75**, 3748 (1995).

[9] D. Weller *et al.*, Phys. Rev. Lett. **75**, 3752 (1995).

[10] H. A. Dürr *et al.*, Science **277**, 213 (1997).

[11] P. Bruno, Phys. Rev. B **39**, 865 (1989). This model has been recently extended by including spin-flip excitations between the majority and minority spin bands: G. van der Laan, J. Phys. Condens. Matter **10**, 3239 (1998).

[12] O. Hjortstam *et al.*, Phys. Rev. B **55**, 15026 (1997).

[13] J. F. Herbst, Rev. Mod. Phys. **63**, 819 (1991), and references therein; *Rare-Earth Iron Permanent Magnetism*, edited by J. M. D. Coey (Clarendon Press, Oxford, 1996).

[14] D. Givord *et al.*, Solid State Commun. **51**, 857 (1984); K. Tokuhara *et al.*, Solid State Commun. **56**, 333 (1985).

[15] A. V. Andreev *et al.*, Sov. Phys. Solid State **27**, 987 (1985).

[16] P. A. Algarabel *et al.*, J. Magn. Magn. Mater. **84**, 109 (1990).

[17] J. Goulon *et al.*, Physica (Amsterdam) **208B**, 199 (1995).

[18] M. Drescher *et al.*, Rev. Sci. Instrum. **68**, 1939 (1997).

[19] J. Vogel and M. Sacchi, Phys. Rev. B **49**, 3230 (1994).

[20] W. L. O'Brien and B. P. Tonner, Phys. Rev. B **50**, 12672 (1994).

[21] C. T. Chen *et al.*, Phys. Rev. Lett. **75**, 152 (1995). The magnetic dipolar operator can be neglected from Eq. (2) since the Fe environments are close to cubic symmetry.

[22] L. Nordström *et al.*, J. Phys. Condens. Matter **25**, 7859 (1993); K. Hummler and M. Faehnle, Phys. Rev. B **53**, 3290 (1996).

[23] B. Szpunar, W. E. Wallace, and J. Szpunar, Phys. Rev. B **36**, 3782 (1987).

[24] D. Givord *et al.*, J. Appl. Phys. **57**, 4100 (1985); D. Givord *et al.*, J. Magn. Magn. Mater. **54–57**, 445 (1986).

[25] H. Onoedera *et al.*, J. Magn. Magn. Mater. **68**, 6 (1987); **68**, 15 (1987).

[26] R. Fruchart *et al.*, J. Phys. F **17**, 483 (1987).

[27] C. Bordel *et al.*, Phys. Rev. B **56**, 8149 (1997).

[28] Details of the orbital to spin ratios for Nd moments calculations will be published elsewhere.

[29] F. Bolzoni *et al.*, J. Magn. Magn. Mater. **66**, 158 (1987).

[30] M. Komelj, O. Grotheer, and M. Fähnle, J. Magn. Magn. Mater. **195**, L275 (1999).

[31] H. Ebert *et al.*, J. Phys. F **18**, L135 (1988).

[32] J. Stankiewicz and J. Bartolomé, Phys. Rev. B **59**, 1152 (1999); Phys. Rev. Lett. **83**, 2026 (1999).

[33] J. Smit, Physica (Utrecht) **21**, 877 (1955); **24**, 39 (1958).